



Title	Indian Ocean Dipole and Rainfall Drive a Moran Effect in East Africa Malaria Transmission
Author(s)	Chaves, Luis Fernando; Satake, Akiko; Hashizume, Masahiro; Minakawa, Noboru
Citation	Journal of Infectious Diseases, 205(12), 1885-1891 https://doi.org/10.1093/infdis/jis289
Issue Date	2012-06-15
Doc URL	http://hdl.handle.net/2115/52659
Rights	This is a pre-copy-editing, author-produced PDF of an article accepted for publication in Journal of Infectious Diseases following peer review. The definitive publisher-authenticated version J Infect Dis. (2012) 205 (12): 1885-1891 is available online at: http://jid.oxfordjournals.org/content/205/12/1885
Type	article (author version)
File Information	JID205-12_1885-1891.pdf



[Instructions for use](#)

1 **Indian Ocean Dipole and Rainfall drive a Moran Effect in East Africa Malaria**
2 **transmission**

3 Luis Fernando Chaves^{1,2*}, Akiko Satake¹, Masahiro Hashizume³, and Noboru Minakawa³

4 ¹Graduate School of Environmental Sciences and Global Center of Excellence program on
5 Integrated Field Environmental Science, Hokkaido University, Sapporo, Japan

6 ² Programa de Investigación en Enfermedades Tropicales, Escuela de Medicina Veterinaria,
7 Universidad Nacional, Heredia, Costa Rica

8 ³Institute of Tropical Medicine (NEKKEN) and Global Center of Excellence program on
9 Tropical and Emergent Infectious Diseases, Nagasaki University, Nagasaki, Japan

10 Short title: **Climate and Moran effect in malaria**

11
12 **Footnote**

13
14 The authors declare no competing interests and that funding agencies had no role on study
15 design.

16
17 **Funding** This work was funded by Japan Society for the Promotion of Science and a Nagasaki
18 University Cooperative Research Grant.

19
20 *corresponding author. Address: Graduate School of Environmental Sciences, Hokkaido
21 University, Room A701 5-chome, Kita 10-jo Nishi, Kita-ku, Sapporo 060-0810, Hokkaido,
22 Japan. Phone: +81-11-706-2267. Fax: +81-11-706-4954. Email: lchaves@ees.hokudai.ac.jp

23
24 Category: **Major Article**

25 197 Words in the abstract

26 3343 words (including: 26 References + Figure Legends)

27 6 Figures + 1 Table

28 Supplementary data:

29 Detailed methods

30

31 **Abstract**

32 **Background:** Patterns of concerted fluctuation in populations, synchrony, can reveal impacts of
33 climatic variability on disease dynamics. Here, we examined whether malaria transmission has
34 been synchronous in an area with a common rainfall regime and sensitive to the Indian Ocean
35 Dipole (IOD), a global climatic phenomenon affecting weather patterns in East Africa.

36 **Methods:** We studied malaria synchrony in five fifteen year long (1984-1999) monthly time
37 series that encompass an altitudinal gradient, ~1000m to 2000m, along Lake Victoria Basin. We
38 quantified the association patterns between rainfall and malaria time series at different altitudes
39 and across the altitudinal gradient encompassed by the study locations.

40 **Results:** We found a positive seasonal association of rainfall with malaria, which decreased with
41 altitude. By contrast, IOD and interannual rainfall impacts on interannual disease cycles
42 increased with altitude. Our analysis revealed a non-decaying synchrony of similar magnitude in
43 both malaria and rainfall, as expected under a Moran effect, supporting a role for climatic
44 variability on malaria epidemics frequency, which might reflect rainfall mediated changes in
45 mosquito abundance.

46 **Conclusion:** Synchronous malaria epidemics call for the integration of knowledge on the forcing
47 of malaria transmission by environmental variability to develop robust malaria control and
48 elimination programs.

49 **Key-words:** Synchrony, Climate Change, Indian Ocean Dipole, *Anopheles*, *Plasmodium*, Time
50 Series

51 Synchrony, the degree of concerted fluctuations among populations in a region, is a key
52 parameter to understand impacts of climatic trends and variability on population dynamics [1].
53 For infectious diseases, synchrony has become especially important because its estimation offers
54 a mean to test hypothesis regarding the importance of exogenous epidemic drivers. In a relatively
55 homogenous environment, a synchrony decay with distance implies that impacts of climatic
56 trends and variability, if any, are marginal when compared with regulatory factors related to
57 population processes, e.g., immunity in diseases, and independent of the changing environment
58 [2]. By contrast, a non-decaying synchrony, of magnitude slightly larger, or similar, to that of the
59 environment, will support a Moran effect, where transmission patterns in a region could be
60 similar by a common mechanism of action for the exogenous, often climatic, forcing [3]. As
61 originally defined, the Moran effect arises by the emerging synchronization of autoregressive
62 dynamics of time series by the impact of common sources of exogenous forcing, i.e., the
63 autonomous (or endogenous) dynamics of a population get tuned to that of external factors
64 influencing the dynamics of populations living under a similar (or correlated) environment [2].

65 Vector-borne diseases, such as malaria, are excellent model systems to study synchrony and test
66 Moran effects. For example, Moran effects are expected in malaria because of the monotonic
67 relationship between vector abundance and transmission [4], and between vectors and rainfall
68 [5]. Lake Victoria basin (LVB) is a unique setting to study exogenous forcing in malaria
69 transmission because of three main reasons: (i) it encompasses an altitudinal gradient, which is
70 also a gradient of malaria endemicity [6, 7]; (ii) it has relatively homogeneous rainfall patterns
71 [8]; (iii) rainfall and malaria are impacted by global climatic phenomena, especially the Indian
72 Ocean Dipole, an irregular oscillation of sea-surface temperatures in which the western Indian
73 Ocean becomes alternately warmer and then colder than the eastern part of the ocean [9, 10].

74 Here, we studied malaria synchrony in five fifteen year long (1984-1999) monthly time series
75 (Fig. 1A) from Lake Victoria basin, West Kenya (Fig. 2). We also studied rainfall time series
76 (Fig. 1B) synchrony to test the condition of environmental autocorrelation necessary for a Moran
77 effect. We used the dipole mode index, DMI, (Fig. 1C) as an IOD index [11] to quantify its role
78 as interannual driver of malaria and rainfall dynamics. We found that both rainfall and malaria
79 had a non-decaying synchrony with distance, and that malaria synchrony was slightly larger than

80 rainfall synchrony, as expected under a Moran effect. A more detailed time scale analysis of
81 synchrony showed that seasonal cycles in malaria transmission were led by two month lagged
82 changes in rainfall, with decreasing intensity as a function of altitude. By contrast, interannual
83 cycles in the disease were driven by IOD, with an increasing intensity with altitude. These
84 patterns could be related to the population dynamics of *Anopheles* mosquitoes, whose abundance
85 is likely driven by rainfall patterns in the region [5, 12]. Finally, our results clearly show that
86 patterns of climatic variability have a strong signature in malaria transmission among vulnerable
87 populations, and are, therefore, a necessary input for a strong malaria control/elimination
88 framework.

89 **Materials and Methods**

90 **Data** Malaria and rainfall data spanned from January 1985 to December 1999. The five malaria
91 time series were monthly counts of inpatients admitted into the hospitals because of high fever
92 and other clinical malaria symptoms. In Kericho, all malaria cases were confirmed by blood slide
93 examination [13]. In the other four sites (Maseno, Kendu Bay, Kisii and Kapsabet) we collected
94 the data from books with malaria diagnosed inpatient records. Unfortunately, these books did not
95 indicate whether all recorded malaria cases were confirmed by blood slide examination.
96 However, we were informed by staff members from each hospital that cases were often
97 confirmed by blood slide examination. We restricted our samples to this kind of malaria
98 infections, i.e., inpatient admissions, in order to make a sound statistical analysis at the price of
99 using data that likely underestimate the total number of malaria infections [14]. Rainfall data
100 were obtained from the Kenyan Meteorological service. We use rainfall records from some of
101 the same locations of the malaria time series and a location midway between the two lowest
102 altitude sites (Fig. 2). Specifically, we employ meteorological records from Kisumu as proxy
103 inputs for Kendu Bay and Maseno, localities for which we were unable to find relatively
104 complete records through the Kenyan Meteorological services and other meteorological data
105 repositories. We chose Kisumu because of the lack of missing observations during the study
106 period, and by the similar rainfall patterns to Kendu Bay and Maseno according to
107 meteorological models [8].

108 **Statistical Analysis** To estimate synchrony in the time series first we removed non-stationary
109 trends [15] in the malaria time series(Fig. 1D) using three standard procedures: local polynomial
110 regression fitting (Loess) [15], singular spectrum analysis (SSA) [16] and the empirical mode
111 decomposition (EMD) [17]. These methods have different assumptions and outcomes, Loess
112 extracts (non)linear trends (Fig. 1E), while SSA (Fig. 1F) and EMD decompose signals into
113 different oscillatory (Fig. 1G, 1H and 1I) and non-cyclical components. In SSA the trends are
114 extracted by examining the variability of the largest eigenvalue from an autocovariance matrix,
115 while EMD decomposes a time series by building oscillatory signals, Intrinsic Mode Functions
116 (IMF), that are repeatedly subtracted from the time series. We employed these different methods
117 to ensure robustness in the inferences from subsequent analyses. The lack of non-stationary
118 trends in rainfall made unnecessary the treatment with Loess and SSA. However, we
119 decomposed rainfall data using EMD to perform frequency specific association analysis (Fig. 3).
120 Second, we estimated the synchrony, r_0 , i.e., cross correlation at lag 0, of rainfall and detrended
121 malaria time series, using both linear regression [2] and spline correlogram on high frequency
122 filtered, detrended time series [18]. Third, we studied the association between rainfall and DMI
123 with malaria along the altitudinal gradient of our study locations using cross correlation
124 functions [15]. Further details about the data and methods are presented in the Supplementary
125 Data.

126 **Results**

127 Estimates for malaria regional synchrony (Table 1) were similar using SSA, Loess (Fig. 4A) and
128 EMD (Fig. 4B) detrended time series. Malaria time series synchronicity was observed across the
129 2-dimensional distance, and altitude, gradients, with all series in phase and with their maximum
130 correlation observed at lag 0 (Fig. 4C), with minimum correlations well above 0.3 at lag 0 in the
131 EMD detrended malaria data (Fig 4B, 4C, Table 1). For rainfall, synchrony estimates from the
132 raw time series (Fig. 4D) and EMD (Fig. 4E) were very similar across the range of distances and
133 altitudes studied (Fig. 4F). To estimate the smoothed correlogram of malaria (Fig. 4B) and
134 rainfall (Fig. 4E) we employed only the EMD detrended time series since this procedure also
135 allowed to filter out high frequency components in the time series, which can artificially increase
136 time series synchrony by the emerging correlation expected from high frequency band

137 constraints. The smoothed correlograms for both malaria (Fig. 4B) and rainfall (Fig. 4E) were
138 similar to the regional synchrony, as the 95% confidence envelope contained the smoothed
139 correlogram along the range of studied distances in each case (Fig. 4B, 4E). Similarly, as
140 expected under a Moran effect, the regional malaria and rainfall synchrony patterns were not
141 statistically different (Table 1). Two-month lagged rainfall had the highest positive correlation
142 with malaria, with a decreasing association as function of increasing elevation (Fig. 5A), a
143 pattern also observed for an analysis based only on the EMD extracted seasonal malaria IMFs
144 (Fig. 5B). The consideration of EMD extracted interannual malaria IMFs (Fig. 5C) showed the
145 association between interannual rainfall and interannual malaria to have a maximum positive
146 correlation when rainfall is 1 month lagged in relation with malaria, and a maximum negative
147 correlation when rainfall is 4 month lagged in relation with malaria, suggesting a role for rainfall
148 temporal variability in the synchronous malaria dynamics. The SSA detrended Malaria-DMI
149 Cross Correlation Function (Fig. 5D) showed the positive association between these time series
150 was maximum for up to 4 months of lagged DMI at altitudes over 1600 m. When the seasonal
151 (Fig. 5E) and interannual (Fig. 5F) malaria IMF were correlated with DMI, the association up to
152 4 months of lagged DMI showed to be robust at interannual scales and altitudes over 1600 m. In
153 addition, the analysis with the IMFs also showed that DMI and seasonal components of malaria
154 are associated at seasonal scales for 3 and 4 months of lagged DMI (Fig. 5E) and the association
155 between DMI and malaria can be continuous along the altitudinal gradient given the emergence
156 of significant patterns of association at altitudes below and above 1600 m (Fig. 5F). Patterns of
157 association between malaria and DMI could be mediated by the impact of DMI on rainfall.
158 DMI and rainfall have a correlation that decreases with altitude, which is maximized between 2
159 and 6 months (Fig. 6A), where DMI has nil impacts on the seasonal components of rainfall (Fig.
160 6B), but is positively associated with the interannual components of rainfall (Fig. 6C).

161

162 **Discussion**

163 Moran effects have seldom been observed in population dynamics [2, 3]. This could reflect the
164 dominance of endogenous feedbacks over exogenous forcing in population dynamics [19]. For
165 example, in diseases, a decaying synchrony with distance, or travelling waves of transmission,

166 have been described for both vector-borne diseases [20] and directly transmitted diseases [21]. In
167 contrast, we found that both seasonal and interannual cycles of malaria have a non-decaying
168 synchrony, both in 2-d distance and along an altitudinal gradient, at distances far greater than
169 mosquito vector dispersal, which on average barely exceeds 2 km [22] or children movement in
170 the area [23]. Moreover, the degree of synchrony in malaria time series is slightly above, yet not
171 statistically different, from rainfall synchrony, as expected under a Moran effect [3].

172 A Moran effect in malaria transmission at the LVB could be explained by the monotonic
173 dependence of *Plasmodium* parasite transmission on *Anopheles* vector density in endemic areas
174 [4]. Mosquito population regulation is sensitive to the availability and stability of larval habitats
175 [5, 24]. In fact, *Anopheles* vector density tracks rainfall variability in LVB in a regular fashion
176 [12]. It takes about two months for malaria transmission to reach its peak following large rainfall
177 events, roughly the total time of a few mosquito generations [25] including the parasite
178 incubation period [26]. This probably implies a reactive response by mosquitoes to the transient
179 creation of habitats by rainfall, assuming a density-dependent regulation [14], a pattern described
180 in other species of mosquitoes vector of pathogens. Since *Anopheles* mosquitoes are ubiquitous
181 in LVB [5, 12, 24], a synchronized amplification of their populations and malaria transmission
182 following rainfall could explain the patterns of synchrony we report here. If this is the case, then
183 the IOD, which has the strongest impact on rainfall at high altitudes according to climatic
184 circulation models [8], could drive the Moran effect in malaria transmission along LVB probably
185 by homogenizing rainfall synchrony across the altitudinal gradient, thus homogenizing weather
186 conditions that increase mosquito productivity [24]. The existence of Moran effects in malaria
187 transmission is a pattern that shows the non-trivial impacts of climatic variability on malaria
188 epidemics. For example, the spatial extent of synchronous patterns in malaria transmission, i.e.,
189 the maximum distance over which malaria synchrony is constant, could be used as indicator of
190 the minimum spatial scale for interventions aimed at eliminating malaria from a given landscape.
191 Thus, consideration of impacts by environmental variability on malaria transmission biology is
192 required to increase robustness in the development and implementation of malaria control and
193 elimination programs, to at least be prepared against surprises that can arise from climatic
194 variability, one of the many aspects shaping the complexity of malaria transmission.

195

196 **References**

- 197 1. Liebhold A, Koenig WD, Bjørnstad ON. Spatial synchrony in population dynamics. Annual Review of
198 Ecology Evolution and Systematics **2004**; 35:467-490.
- 199 2. Ranta E, Lundberg P, Kaitala V. Ecology of Populations. Cambridge: Cambridge University Press, **2006**.
- 200 3. Blasius B, Stone L. Ecology: Nonlinearity and the Moran effect. Nature **2000**; 406:846-847.
- 201 4. Smith DL, Drakeley CJ, Chiyaka C, Hay SI. A quantitative analysis of transmission efficiency versus
202 intensity for malaria. Nat Commun **2010**; 1:108.
- 203 5. Fillinger U, Sonye G, Killeen GF, Knols BGJ, Becker N. The practical importance of permanent and
204 semipermanent habitats for controlling aquatic stages of *Anopheles gambiae sensu lato* mosquitoes:
205 operational observations from a rural town in western Kenya. Tropical Medicine & International Health
206 **2004**; 9:1274-1289.
- 207 6. Drakeley CJ, Carneiro I, Reyburn H, et al. Altitude-Dependent and -Independent Variations in
208 *Plasmodium falciparum* Prevalence in Northeastern Tanzania. Journal of Infectious Diseases **2005**;
209 191:1589-1598.
- 210 7. Bødker R, Msangeni HA, Kisinza W, Lindsay SW. Relationship between the intensity of exposure to
211 malaria parasites and infection in the Usambara Mountains, Tanzania. American Journal of Tropical
212 Medicine and Hygiene **2006**; 74:716-723.
- 213 8. Anyah R, Semazzi F, Xie L. Simulated physical mechanisms associated with multi-scale climate
214 variability over Lake Victoria Basin in East Africa. Monthly Weather Review **2006**; 134:3588-3609.
- 215 9. Hashizume M, Terao T, Minakawa N. The Indian Ocean Dipole and malaria risk in the highlands of
216 western Kenya. Proceedings of the National Academy of Sciences of the United States of America **2009**;
217 106:1857-1862.
- 218 10. Behera SK, Luo J-J, Masson S, et al. Paramount impact of the Indian Ocean Dipole on the East African
219 short rains: A CGCM Study. J Climate **2005**; 18:4514-4530.
- 220 11. Saji NH, Goswami BN, Vinayachandran PN, Yamagata T. A dipole mode in the tropical Indian Ocean.
221 Nature **1999**; 401:360-3.
- 222 12. Minakawa N, Sonye G, Mogi M, Githeko A, Yan GY. The effects of climatic factors on the distribution
223 and abundance of malaria vectors in Kenya. J Med Entomol **2002**; 39:833-841.
- 224 13. Shanks G, Biomndo K, Hay S, Snow R. Changing patterns of clinical malaria since 1965 among a tea
225 estate population located in the Kenyan highlands. Transactions of the Royal Society of Tropical
226 Medicine and Hygiene **2000**; 94:253 - 255.
- 227 14. Chaves LF, Koenraadt CJM. Climate Change and Highland Malaria: Fresh Air for a Hot Debate. The
228 Quarterly Review of Biology **2010**; 85:27-55.
- 229 15. Shumway RH, Stoffer DS. Time series analysis and its applications. New York: Springer, **2000**.
- 230 16. Ghil M, Allen MR, Dettinger MD, et al. Advanced spectral methods for climatic time series. Reviews
231 of Geophysics **2002**; 40.
- 232 17. Huang NE, Shen Z, Long SR, et al. The empirical mode decomposition and the Hilbert spectrum for
233 nonlinear and non-stationary time series analysis. Proceedings of the Royal Society of London Series a-
234 Mathematical Physical and Engineering Sciences **1998**; 454:903-995.
- 235 18. Bjørnstad ON, Falck W. Nonparametric spatial covariance functions: Estimation and testing.
236 Environmental and Ecological Statistics **2001**; 8:53-70.
- 237 19. Turchin P. Complex population dynamics. Princeton: Princeton University Press, **2003**.
- 238 20. Cummings DAT, Irizarry RA, Huang NE, et al. Travelling waves in the occurrence of dengue
239 haemorrhagic fever in Thailand. Nature **2004**; 427:344-347.

- 240 21. Viboud C, Bjørnstad ON, Smith DL, Simonsen L, Miller MA, Grenfell BT. Synchrony, waves, and spatial
241 hierarchies in the spread of influenza. *Science* **2006**; 312:447-451.
- 242 22. Silver JB. *Mosquito ecology: field sampling methods*. 3rd ed. New York: Springer, **2008**.
- 243 23. Prothero RM. *Migrants and Malaria*. London (UK): Longmans, **1965**.
- 244 24. Minakawa N, Omukunda E, Zhou G, Githeko A, Yan G. Malaria vector productivity in relation to the
245 highland environment in Kenya. *American Journal of Tropical Medicine and Hygiene* **2006**; 75:448-53.
- 246 25. Bayoh MN, Lindsay SW. Effect of temperature on the development of the aquatic stages of
247 *Anopheles gambiae sensu stricto* (Diptera : Culicidae). *Bulletin of Entomological Research* **2003**; 93:375-
248 381.
- 249 26. Lindsay SW, Birley MH. Climate change and malaria transmission. *Annals of Tropical Medicine and*
250 *Parasitology* **1996**; 90:573-588.

251

252 **Acknowledgements**

253 We thank R. Snow for providing hospital and meteorological data for Kericho. We also thank the
254 staff at the Kendu Bay, Maseno, Kisii and Kapsabet hospitals for their help with data
255 compilation. LFC, MH and NM had grant support to study synchrony patterns on malaria
256 transmission at Lake Victoria Basin. LFC is a Gaikokuujin Fellow of Japan Society for the
257 Promotion of Science.

258

259 **Figure Legends**

260 **Fig. 1 Data** (A) Malaria Time Series. (B) Rainfall. (C) Dipole Mode Index. (D) Trends (solid
 261 lines for Loess, dashed lines for Singular Spectrum Analysis [SSA] and dotted lines for
 262 Empirical Mode Decomposition[EMD]). There is no dashed line for Kisii and Kapsabet because
 263 the SSA was unable to detect any trends. (E) Loess detrended Malaria time series. (F) SSA
 264 detrended Malaria Time Series. (G) Malaria intrinsic mode functions, IMFs, with interannual
 265 cycles. (H) Malaria IMFs with seasonal cycles. (I) Malaria IMFs with high frequency cycles.
 266 Inset legends identify time series with colors. Color codes are shared by panels A, D, E, F, G, H,
 267 I. IMFs were derived via an EMD for each time series.

268 **Fig. 2 Study Sites in Lake Victoria Basin, Western Kenya.** Kisumu ($0^{\circ}6'S$ $34^{\circ}45'E$ Atltitude =
 269 1131 m); Kendu Bay ($0^{\circ}24'05''S$, $34^{\circ}39'56''E$, Altitude = 1240 m); Maseno ($0^{\circ}00'15''S$,
 270 $34^{\circ}36'16''E$, Altitude = 1500 m); Kisii ($0^{\circ}40'S$, $34^{\circ}46'E$, Altitude = 1670 m); Kapsabet ($0^{\circ}12'N$,
 271 $35^{\circ}06'E$, Altitude = 2000 m); Kericho ($0^{\circ}23'55''N$, $35^{\circ}15'30''E$, Altitude = 2000 m). In the map
 272 elevation is measured in meters, m, and indicated by gray. Location color indicates the data
 273 available at each site ; blue (rainfall); green (disease) and red (disease and rainfall).

274 **Fig. 3 Rainfall Time Series Empirical Mode Decomposition** (A) Intrinsic mode functions,
 275 IMFs, with interannual cycles; (B) IMFs with seasonal cycles; (C) IMFs with high frequency
 276 cycles. Inset legends identify time series with colors.

277 **Fig. 4 Synchrony Analysis** (A) Malaria time series correlation at lag 0, r_0 , as function of latitude
 278 (Lat), longitude (Long) and two-dimensional distance [2D] between the studied localities. Colors
 279 indicate the method employed to detrend the malaria time series employed to estimate r_0 . (B) 2D
 280 distance spline correlogram (3 edf) for the signal obtained by adding the seasonal and interannual
 281 intrinsic mode functions from the empirical mode decomposition applied to the malaria time

282 series (C) Contour maps for temporal cross-correlations between the Empirical Mode
 283 Decomposition [EMD] detrended malaria time series (D) Rainfall time series correlation at lag 0,
 284 r_0 , as function of latitude (Lat), longitude (Long) and 2D distance between the studied localities.
 285 (E) 2D distance spline correlogram (2 edf) for the signal obtained by adding the seasonal and
 286 interannual intrinsic mode functions from the empirical mode decomposition applied to the
 287 rainfall time series. (F) Contour maps for temporal cross-correlations among the Rainfall time
 288 series. In A, B, D, and E Synch is the estimated regional synchrony obtained with each method.
 289 In B and E dotted lines indicate the 95% confidence envelope for the smoothed correlation
 290 function, solid line, obtained with 1000 data permutations. In C and F, the y axis represents the
 291 lag for the cross correlation and the x axis represents the 2D distance. Values in the contour lines
 292 are correlations, which are significantly different from 0 when their absolute value is above
 293 0.075 ($P < 0.05$).

294 **Fig. 5 Time scale impacts of Rainfall and Indian Ocean Dipole on malaria synchrony across**
 295 **an altitude gradient** (A) Singular Spectrum analysis detrended malaria time series (SSA
 296 Malaria) correlation with Rainfall (B) Seasonal malaria Intrinsic Mode Function, IMF,
 297 correlation with Seasonal Rainfall IMF (C) Interannual malaria IMF correlation with Interannual
 298 Rainfall IMF (D) SSA detrended malaria correlation with Dipole mode index (DMI) (E)
 299 Seasonal malaria IMF, correlation with DMI (F) Interannual malaria IMF correlation with DMI.
 300 IMFs for each malaria time series were obtained by empirical mode decompositions. In all
 301 panels the x axis represents the lag for the cross correlation and the y axis represents the site
 302 altitude. Values in the contour lines are correlations, which are significantly different from 0
 303 when their absolute value is above 0.075 ($P < 0.05$).

304 **Fig. 6 Time Scale association between Rainfall and Dipole mode Index (DMI).** (A) Rainfall
305 correlation with DMI (B) Seasonal rainfall Intrinsic Mode Function, IMF, correlation with DMI
306 (C) Interannual rainfall IMF, correlation with DMI. IMFs for each malaria time series were
307 obtained by empirical mode decompositions. The x axis represents the lag for the cross
308 correlation and the y axis represents the site altitude. Values in the contour lines are correlations,
309 which are significantly different from 0 when their absolute value is above 0.075 ($P < 0.05$).

Figure 1
[Click here to download high resolution image](#)

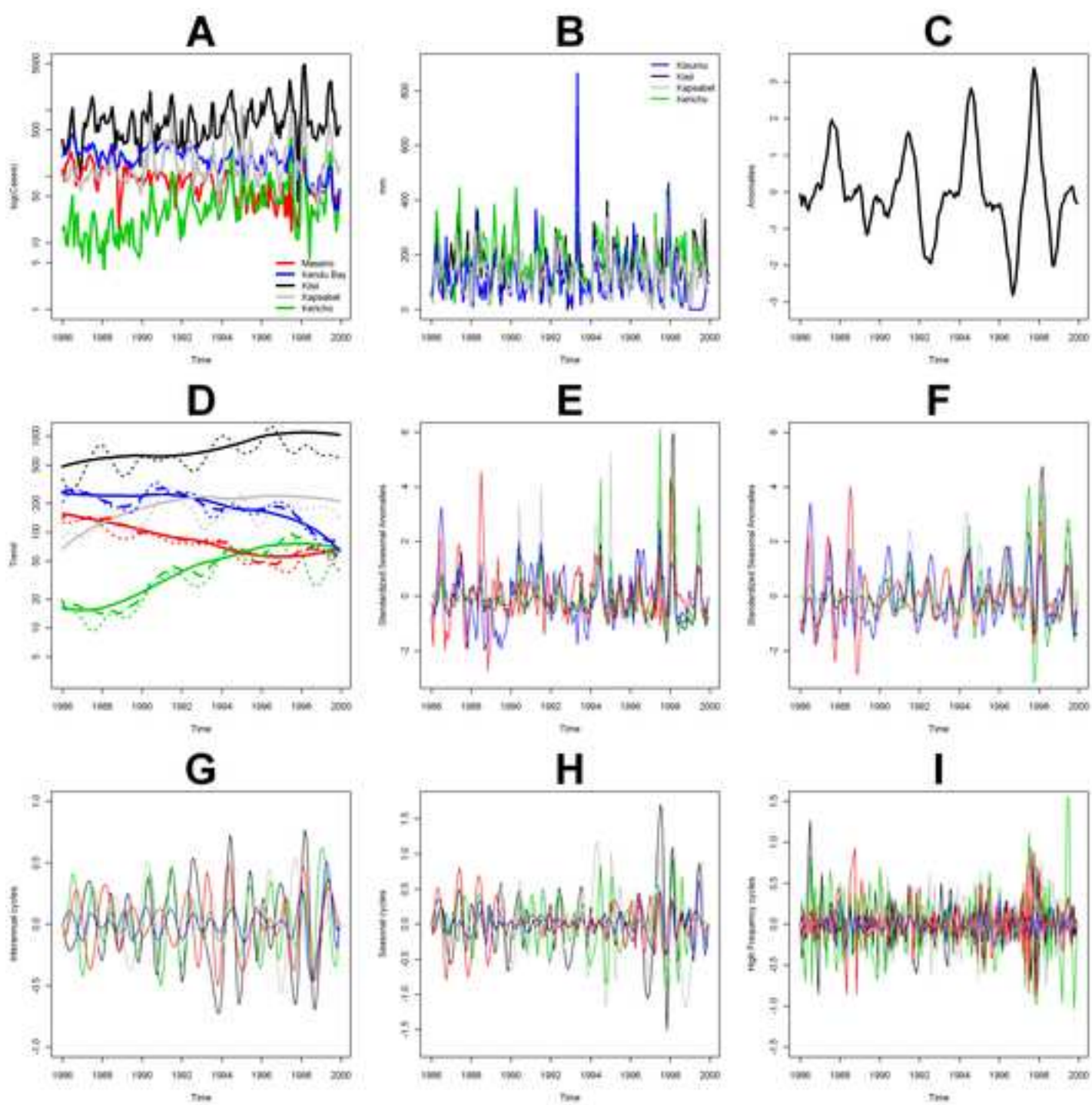


Figure 2
[Click here to download high resolution image](#)

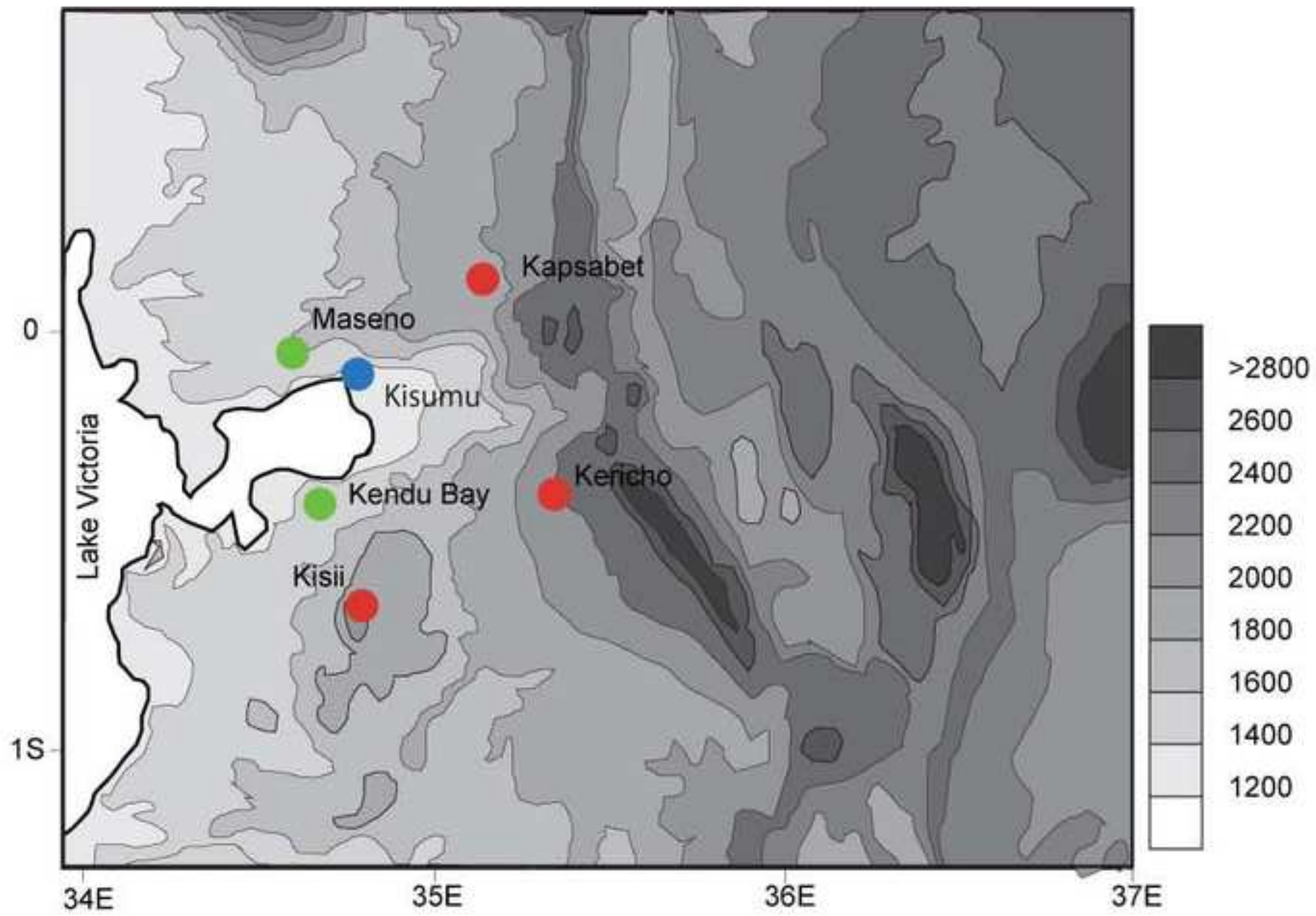


Figure 3
[Click here to download high resolution image](#)

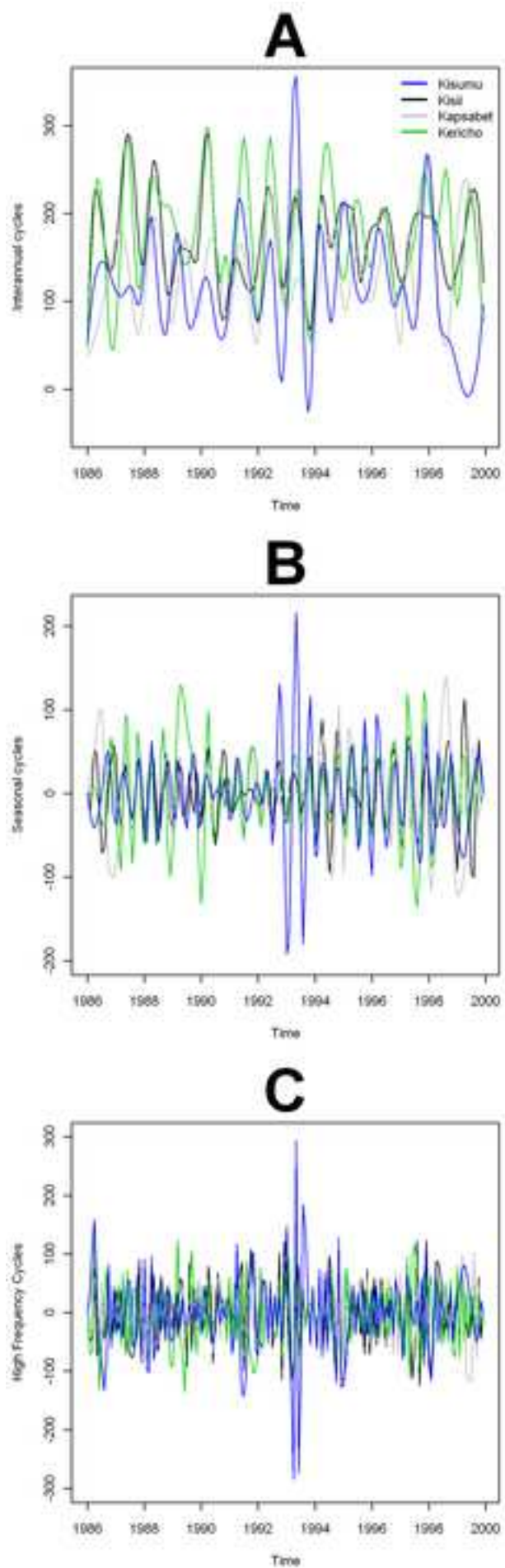


Figure 4
[Click here to download high resolution image](#)

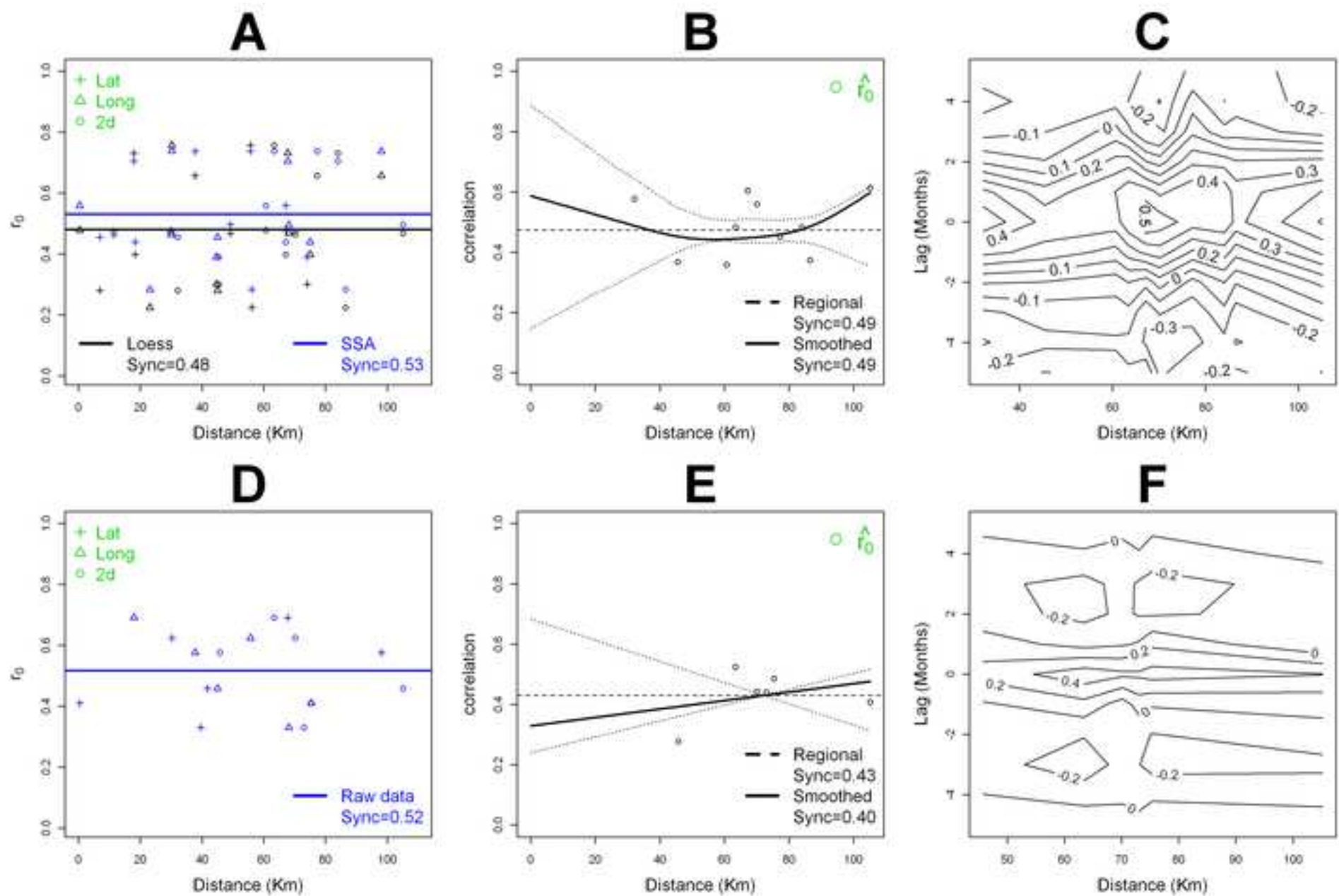


Figure 5
[Click here to download high resolution image](#)

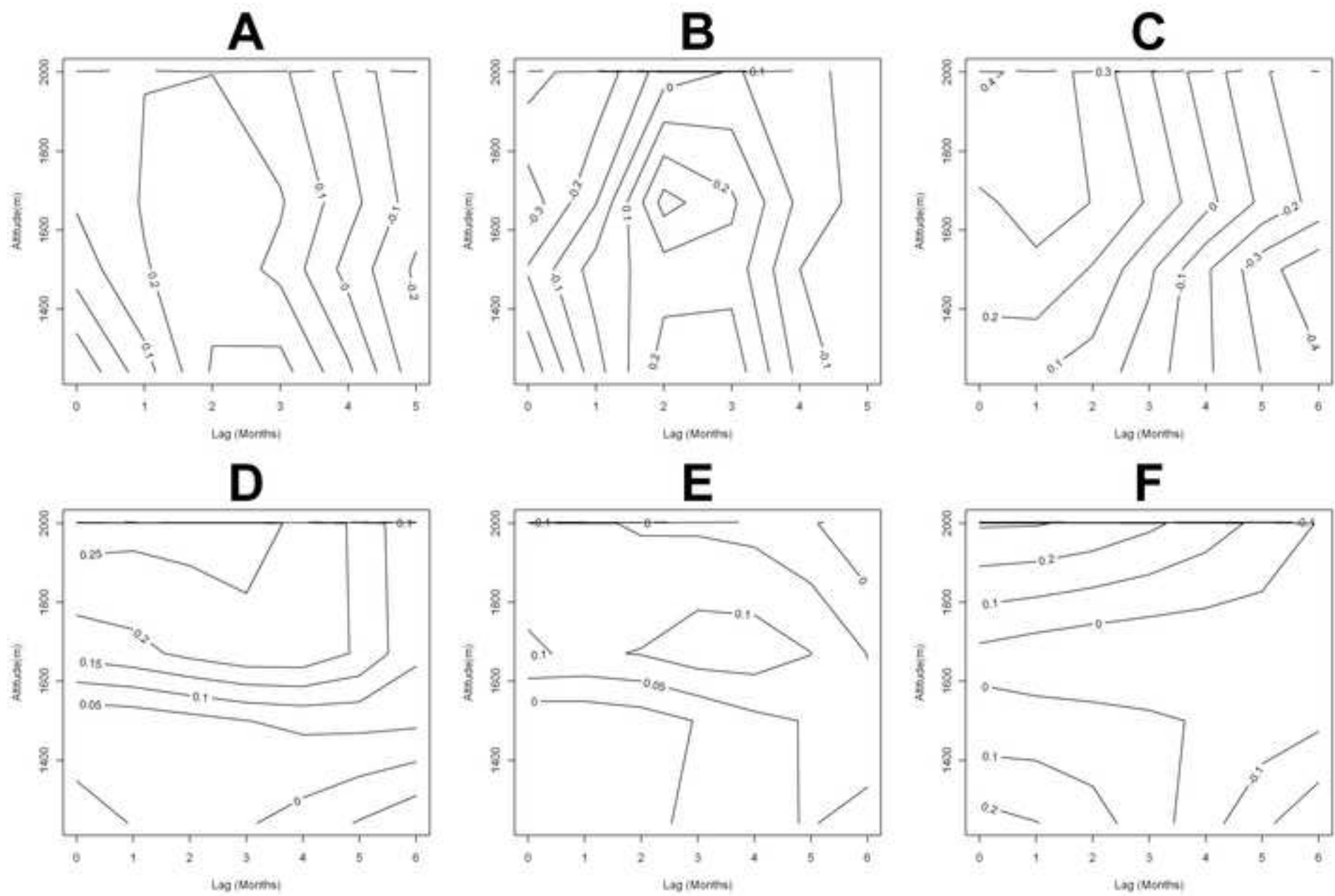


Figure 6
[Click here to download high resolution image](#)

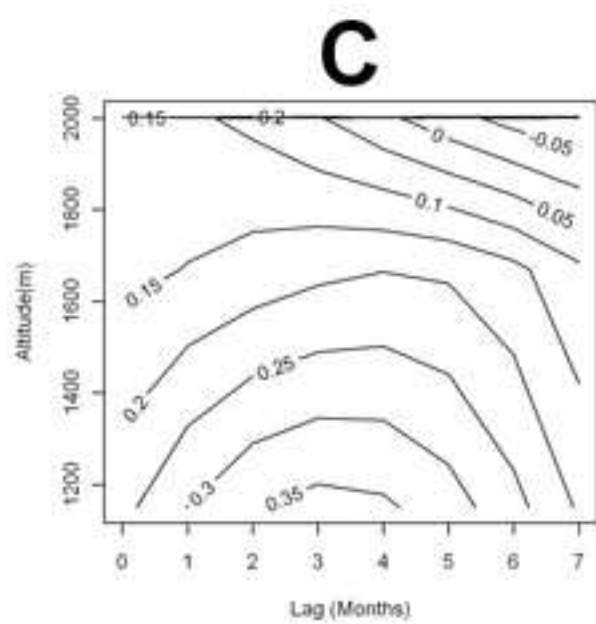
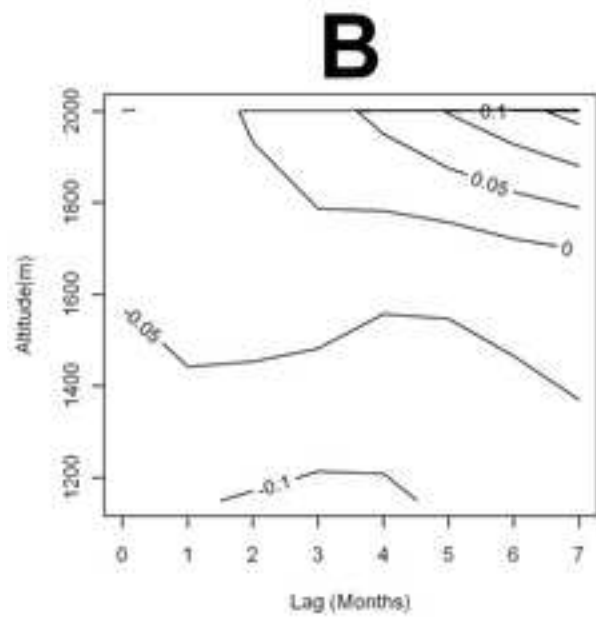
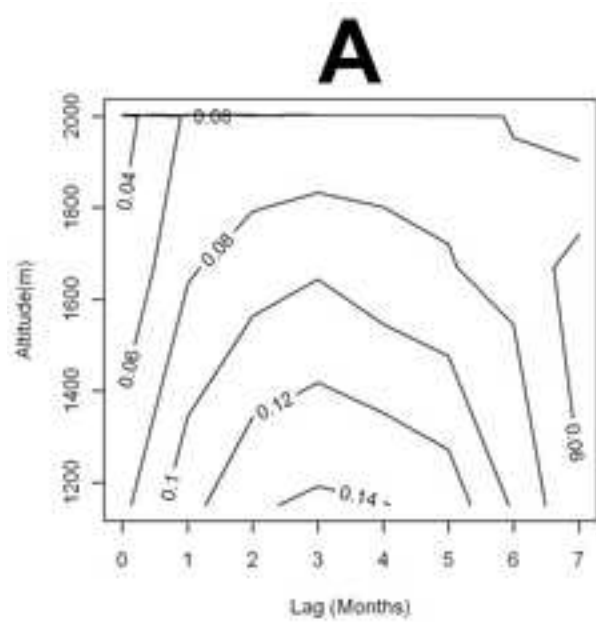


Table 1. Confidence limits for the regional synchrony estimates. 95% confidence limits were estimated from the standard error of maximum likelihood estimates for the regional synchrony.

Time Series	Mean \pm S.E.	95% Confidence limits
Malaria-LOESS	0.48 ± 0.06	0.34 - 0.61
Malaria-SSA	0.53 ± 0.05	0.42 - 0.64
Malaria-EMD	0.49 ± 0.03	0.42 - 0.56
Rainfall-Raw Data	0.52 ± 0.06	0.37- 0.66
Rainfall-EMD	0.43 ± 0.03	0.34 - 0.51

Supplementary data

Detailed Methods

Software

All statistical analyses were performed using the statistical software R[1].

Time series detrending methods

Loess

This is a well established procedure to remove non-linear trends from time series data [2]. A non-parametric trend is fitted to the time series using local polynomials regression fits, Loess, which is then subtracted from the original series [3]. For the synchrony analysis, such residuals are then standardized to be normal and with a variance of one [2].

Singular spectrum analysis (SSA)

This non-parametric technique separates trends and oscillatory components from noise in a time series [4]. The method consists in the computation of the eigenvalues and eigenvectors from a covariance matrix [**M**] whose element m_{ij} is the covariance between lags i and j . The projection of the time series on the eigenvectors (the principal components of the matrix) reconstructs the pattern of variability associated with the selected eigenvalue, resulting in a de-noised time series [4]. The eigenvalues themselves indicate how much variance is accounted for by the different components [4].

Empirical Mode Decomposition (EMD)

This technique decomposes time series into trends and oscillatory components. Briefly, a time series goes through an iterative sifting process which decomposes the time series into a sum of intrinsic mode functions (IMF). The algorithm to extract IMFs is as follows: (i) Envelopes are built by joining through a cubic spline all the maxima (upper envelope) and minima (lower envelope); (ii) the mean of the two envelopes is subtracted from the time series; and (iii) the

process is repeated until an IMF is obtained. IMFs should satisfy the assumption of a narrow band (which is fulfilled when the number of zero crossings and extrema are either equal or differ by one) and the mean of its upper and lower envelopes, equals zero (which renders impossible unwanted fluctuations expected by asymmetric waveforms). The process of extracting IMFs can be repeated on the residuals from each IMF extraction until all cyclic components are extracted and the final residuals represent a trend for the data. Further details and a mathematically rigorous explanation are presented by Huang et al [5]. Regarding our data, we extracted three IMFs and the trend (Fig. 1D) from the malaria time series, each IMF corresponding to interannual cycles (Fig. 1G), seasonal cycles (Fig. 1H) and high frequency cycles (Fig. 1I). For the rainfall time series we only extracted two IMFs, because the extraction of a third IMF did not lead to the separation of trends, and the trends lacked any noticeable non-cyclical pattern (Fig. 3A). Like the malaria time series, the rainfall time series also had seasonal (Fig. 3B) and high frequency components (Fig. 3C). For the EMD malaria data were log-transformed, in order to minimize signal interference.

Spline Correlogram

We employed spline correlograms to study rainfall and malaria synchrony. This technique can be used to study the spatio-temporal autocorrelation among populations. Basically, smoothing splines are used to generate a functional correlogram, i.e., an assumption free and smooth function depicting spatial autocorrelation, among several time series, which depends on distance. Given the low number of time series, (5 for malaria and 4 for rainfall, numbers rendering impossible a bootstrap), we generated a null distribution from the estimator by computing spline correlograms from random time series. The random time series were constructed by sampling without replacement the detrended, and also high frequency filtered, time series, i.e., we analyzed time series without trends to ensure a stationary mean and, series without high frequency components to avoid the spurious correlations that can be expected when these components are considered. This procedure was repeated 1000 times to extract the 2.5% and 97.5 % quantiles of the null distribution, which correspond to the 95% confidence envelope of the spline correlogram [6]. For the smoothing of the 5 malaria time series we employed 3 degrees of freedom (edf), and to make a reliable comparison we used 2 edf given that we only had 4 rainfall time series.

Cross Correlation Function

Cross correlation function, CCF, is formally defined as the ratio between the cross-covariance function of two time series divided by the square root of the product of each series variance, and represents the association between time series as function of time [2].

References

1. R DCT. R: A language and environment for statistical computing
Vienna, Austria: R Foundation for Statistical Computing, **2011**.
2. Shumway RH, Stoffer DS. Time series analysis and its applications. New York: Springer, **2000**.
3. Ranta E, Lundberg P, Kaitala V. Ecology of Populations. Cambridge: Cambridge University Press, **2006**.
4. Ghil M, Allen MR, Dettinger MD, et al. Advanced spectral methods for climatic time series. *Reviews of Geophysics* **2002**; 40.
5. Huang NE, Shen Z, Long SR, et al. The empirical mode decomposition and the Hilbert spectrum for nonlinear and non-stationary time series analysis. *Proceedings of the Royal Society of London Series a-Mathematical Physical and Engineering Sciences* **1998**; 454:903-995.
6. Bjørnstad ON, Falck W. Nonparametric spatial covariance functions: Estimation and testing. *Environmental and Ecological Statistics* **2001**; 8:53-70.